ACS Chemical Neuroscience pubs.acs.org/acschemicalneuroscience Letter

Dual Effect of Amino Modified Polystyrene Nanoparticles on Amyloid β Protein Fibrillation

Celia Cabaleiro-Lago,*[,†,§] Fiona Quinlan-Pluck,[†] Iseult Lynch,[†] Kenneth A. Dawson,[†] and Sara Linse*[,‡]

[†]Centre for BioNano Interactions, School of Chemistry and Chemical Biology, University College Dublin, Belfield, Dublin 4, Ireland, and [‡]Biochemistry Department, Lund University, PO Box 124, 22100 Lund, Sweden

Abstract

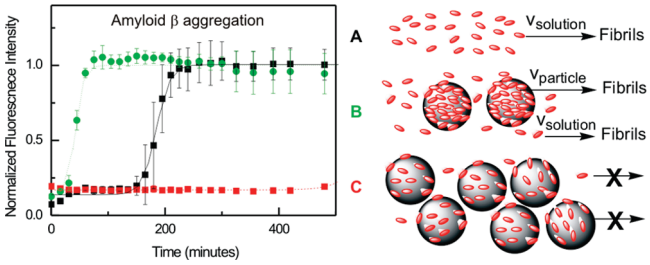

The fibrillation kinetics of the amyloid β peptide is analyzed in presence of cationic polystyrene nanoparticles of different size. The results highlight the importance of the ratio between the peptide and particle concentration. Depending on the specific ratio, the kinetic effects vary from acceleration of the fibrillation process by reducing the lag phase at low particle surface area in solution to inhibition of the fibrillation process at high particle surface area. The kinetic behavior can be explained if we assume a balance between two different pathways: first fibrillation of free monomer in solution and second nucleation and fibrillation promoted at the particle surface. The overall rate of fibrillation will depend on the interplay between these two pathways, and the predominance of one mechanism over the other will be determined by the relative equilibrium and rate constants.

Keywords: Amyloid, aggregation kinetics, nanoparticles

Protein aggregation into amyloid fibrils is a pathological hallmark of many diseases, including Alzheimer's and Parkinson's diseases (*1*). These disorders are caused by, or related to, conformational changes from nontoxic to toxic forms of specific proteins. Fibrillogenesis is a nucleation−growth process leading to the conversion of monomeric amyloidogenic proteins to amyloid fibrils and plaques (*2*). Diverse substances (small molecules and peptides) are known to interfere with the fibrillation process (*3*−*6*). Because many amyloidogenic proteins have a tendency to accumulate at phase boundaries, the process is also largely affected by the presence of biological or foreign surfaces, for example, synthetic nanoparticles (*7*−*9*), dendrimers(*10*), or larger particles(*11*). Interestingly, copolymeric nanoparticles have been found to have opposing effects in different systems with an acceleration of β2-microglobulin (β2m) fibrillation (*7*) and retardation of amyloid β peptide (Aβ) fibrillation (*8*). Specifically in the case of β2m, the presence of nanoparticles leads to a shortening of the lag phase by favoring nucleation of the fibrillation process. This was interpreted to arise from an observed accumulation of β2m at the nanoparticle surface leading to an increased local concentration, which favors oligomerization and the likelihood of formation of critical nuclei for fibrillation (*7*). The retardation observed for Aβ was explained by assuming a tight interaction of the nanoparticles with the monomeric peptide or with growing oligomers, which would deplete the solution concentration or block the growing ends and interfere with their elongation into amyloid fibrils (*8*). Moreover, an influence of the chemical nature of the nanoparticles on the aggregation processes of β2m and Aβ peptide has been reported (*7*−*9*). Other studies show that the folding and therefore the tendency of Aβ peptide to aggregate varies with the chemical nature and charge of the nanoparticle surface (*12*, *13*).

Aβ is the principal protein component of the amyloid plaques found in the later stages of Alzheimer's disease, and extensive data support a central role for Aβ in the disease process. The cytotoxic effects seem to be related to prefibrillar, diffusible assemblies of Aβ that are deleterious to neurons (*14*).

Here we have studied the effect of cationic polymeric nanoparticles on Aβ fibrillation by analyzing the effect of commercial polystyrene particles with amino modification on the *in vitro* aggregation of synthetic Aβ-(1−40) and recombinant Aβ(M1−40) and Aβ(M1−42). The results obtained lead us to hypothesize that there is

Received Date: October 12, 2009
Accepted Date: January 18, 2010
Published on Web Date: January 27, 2010

DOI: 10.1021/cn900027u | *ACS Chem. Neurosci.* (2010), *1*, 279–287

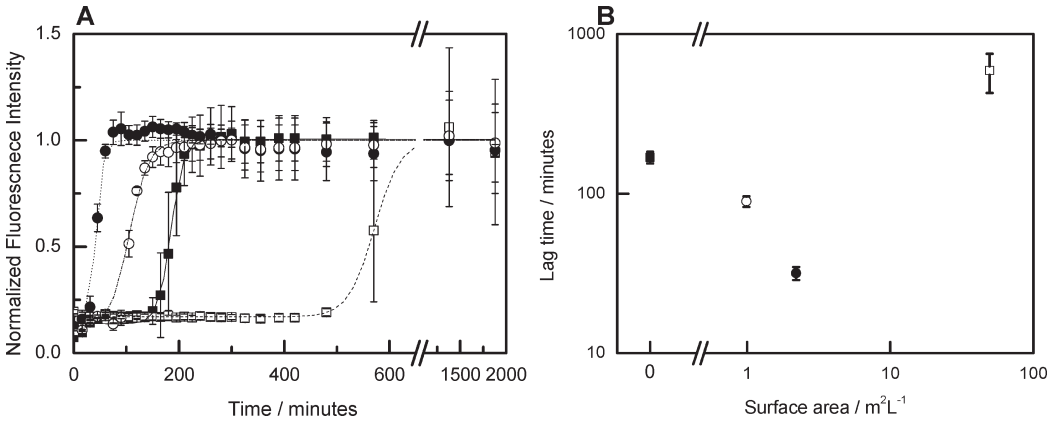

Figure 1. (A) Fibrillation kinetics of Aβ(1−40) (16 μM) at 37 °C monitored by temporal development of ThT fluorescence for different concentrations of 120 nm amine-modified polystyrene nanoparticles: (■) 0, (○) 0.02, (●) 0.05, and (□) 1.1 mg/mL. Lines represent the best fit of eq 1 to the experimental data. (B) Lag times versus nanoparticle surface area in solution from the experiments shown in panel A. Averages and standard deviation over three to six replicates are shown.

a competition between the two different mechanisms of interaction between particles and Aβ, which is tuned by the coverage of the particle surface.

The fibrillation of synthetic Aβ(1−40) *in vitro* is clearly affected by the presence of amino-modified polystyrene nanoparticles. Figure 1 shows the time course of fibrillation followed by means of thioflavin T (ThT) fluorescence. The variation of the ThT fluorescence signal yields information about the extent of amyloid formation (*15*). The fibrillation of Aβ(1−40) in the absence of nanoparticles shows the typical nucleation−elongation profile. A lag phase, indicated by a constant low fluorescence signal (i.e., no highly amyloid-structured species are present) is followed by an elongation phase, during which oligomers grow into fibrils, and finally a steady plateau value after equilibrium is reached. As seen in Figure 1, the presence of nanoparticles essentially affects the lag phase of the fibrillation processes, while the elongation rate remains fairly constant compared with the nanoparticle-free case.

The most striking observation is the dual effect of the amine-modified polystyrene nanoparticles on Aβ fibrillation kinetics. At a constant protein concentration, the fibrillation process is accelerated (shorter lag phase) by nanoparticles at low particle concentration, while at high particle concentration, the fibrillation process is retarded (longer lag phase). While other investigations have seen acceleration of the fibrillation by TiO_2 nanoparticles (*9*) and retardation by dendrimers (*10*) and copolymer particles (*8*), we see both effects for one type of nanoparticle.

Transmission electron images shown in Figure 2 confirm this bimodal (and surprising) picture, showing that after 90 min few amyloid fibrils are observed in solution when no particles or high concentrations of nanoparticles are added. On the other hand, at low particle concentrations, amyloid-like fibrils with the standard

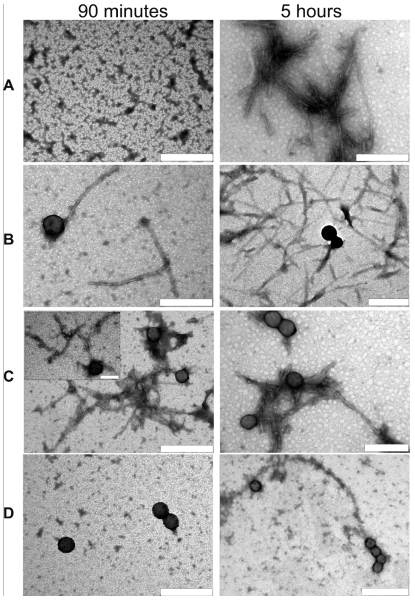

Figure 2. Negatively stained images observed by transmission electron microscopy. Samples were prepared in the absence and presence of different concentrations of 120 nm amine-modified polystyrene nanoparticles: (A) 0, (B) 0.02, (C) 0.05, and (D) 1.1 mg/mL at Aβ(1−40) peptide concentration of 16 μM at two different time points, 90 min and 5 h, of the fibrillation reaction. Scale bar indicates 200 nm. The corresponding ThT development graphs can be seen in Figure 1.

amyloid features (10 nm wide and hundreds of nanometers long) can already be observed after 90 min of incubation of 16 μM Aβ(1−40).

Figure 3 shows fibrillation experiments where nanoparticles are added at different time points after fibrillation has been initiated. In these experiments, we used a high concentration of amine-modified polystyrene nanoparticles (1.1 mg/mL) in the regime causing inhibition of fibrillation when added from the beginning of the kinetic experiment. When added at short times, while

DOI: 10.1021/cn900027u | *ACS Chem. Neurosci.* (2010), *1*, 279–287

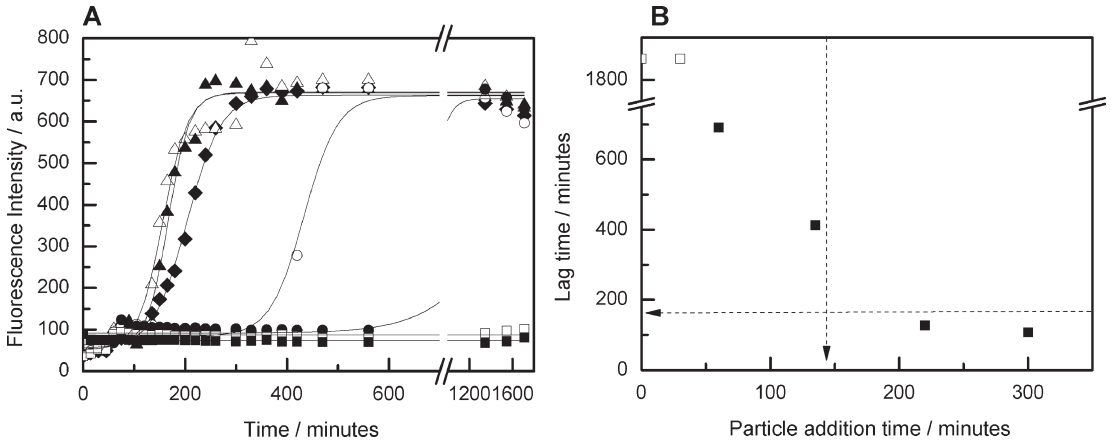

Figure 3. (A) Fibrillation kinetics of Aβ(1−40) at 37 °C monitored by means of ThT fluorescence intensity. Aβ(1−40) (8 μM) was incubated in the absence and presence of 1.1 mg/mL 180 nm polystyrene nanoparticles. Particles were added to the reactions at different times from 0 to 300 min: (♦) no particles; particles added at (■) 0, (□) 30, (●) 60, (○) 135, (▲) 220, and (△) 300 min. Lines are guide to the eye. (B) Lag time values obtained from fitting of eq 1 to the experimental data presented in Figure 3A versus particle addition time. Empty symbols indicate estimated minimum lag times for the shortest addition times. Arrows indicate the corresponding value (min) of lag time in absence of particles. The experiment was repeated two times with similar results.

the process is still in the lag phase, the effect of adding particles is inhibitory. This is reflected as stable low fluorescence values, indicative of no fibril formation. As long as the particles are added before the time point corresponding to the average lag time in the absence of particles (lag time = 138 ± 20 min), the process is inhibited as reflected by prolonged lag times (Figure 3B). In contrast, particles added after the control lag time do not show any significant effects on lag time (see arrows in Figure 3B), indicating that once the critical nuclei are formed the elongation process is so favorable that the interaction between monomer/oligomer and particles cannot overcome it, and thus addition of the amine-modified polystyrene nanoparticles has no impact on the fibrillation process (Figure 3B). Although the interaction between nanoparticles and peptide is strong enough to slow down the fibrillation process at high particle concentration when present from the beginning or added at early times, probably by adsorption of monomeric Aβ or early formed oligomers, the addition of nanoparticles during later stages of the fibrillation process (i.e., once the fibrils have started to form) seems to be incapable of reversing the fibrillation process or destroying the fibrils, as monitored by ThT fluorescence.

The results differ from stopping experiments with Aβ and copolymer nanoparticles, where addition of nanoparticles could revert an ongoing fibrillation process up to a certain time point (*8*), or with IAPP, where addition of copolymer nanoparticles prevented further growth even when the process was in the elongation phase (*16*).

Recombinant Aβ(M1−40) and Aβ(M1−42) were used to analyze the effect of increasing particle concentration for different protein concentrations. We find that the effect exerted by the presence of nanoparticles on the protein fibrillation is clearly dependent on the

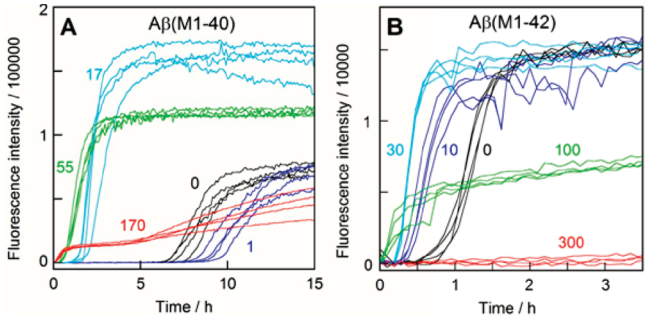

Figure 4. Fibrillation kinetics of recombinant peptides at 37 °C monitored by temporal development of ThT fluorescence for different concentrations of 57 nm amine-modified polystyrene nanoparticles. Four replicates are shown at each condition to illustrate the level of reproducibility: (A) 8 μM Aβ(M1−40) with (black) 0, (blue) 1, (cyan) 17, (green) 55, and (red) 170 μg/mL nanoparticles; (B) 2 μM Aβ(M1−42) with (black) 0, (blue) 10, (cyan) 30, (green) 100, and (red) 300 μg/mL nanoparticles.

concentration ratio between the protein and the particles. The fibrillation of recombinant Aβ(M1−40) or Aβ(M1−42) in the presence of nominally 57 nm amino-modified polystyrene follows the same trend as for Aβ(1−40) (Figure 4). Starting from the pure peptide system (no nanoparticles), after a particle concentration range where no effect is observed (at very low particle concentration), the lag phase is seen to gradually decrease as the nanoparticle concentration is increased. This trend continues until a critical point where the lag-phase vanishes. Hence, fibrillation is accelerated as we increase particle concentration up to a critical point. At even higher nanoparticle concentrations, we observe inhibition of the fibrillation process. Nevertheless, the extent of the inhibition effect depends on the protein/particle concentration ratio. At low peptide concentration, the acceleration regime is reached at quite low particle concentrations,

DOI: 10.1021/cn900027u | *ACS Chem. Neurosci.* (2010), *1*, 279–287

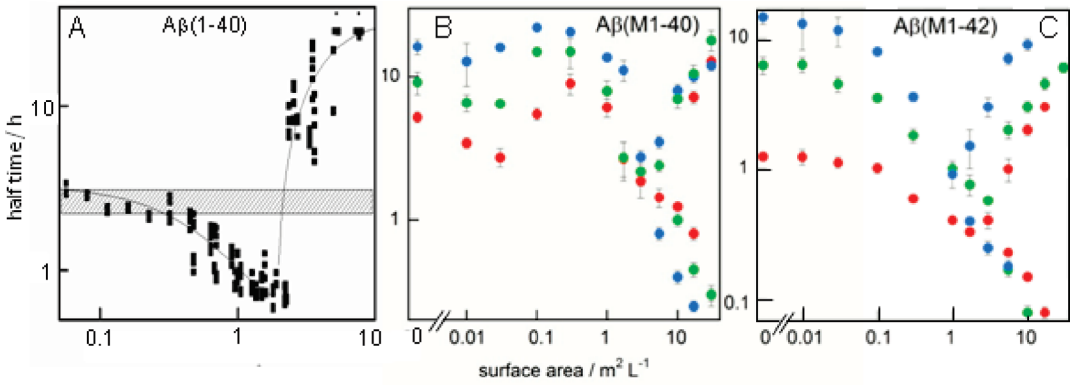

Figure 5. (A) Half-time of fibrillation versus particle surface area in solution for different experiments performed in the presence of 120 and 180 nm polystyrene nanoparticles at a constant concentration of Aβ(1−40) (8 μM). Horizontal bar indicates the half-time value range in the absence of particles. Lines are guide to the eye. Asterisks indicate estimated values in cases where the onset of the fibrillation is observed but the equilibrium plateau is not reached within the time frame of the experiment. (B, C) Half times of fibrillation versus particle surface area in solution in the presence of 57 nm amine-modified polystyrene nanoparticles at (B) (blue) 3, (green) 6, and (red) 8 μM Aβ(M1−40) and (C) (blue) 0.5, (green) 1, and (red) 2 μM Aβ(M1−42). Some fibrillation traces for the recombinant peptides at high nanoparticle concentrations are biphasic, and therefore two values are reported for the half-time. In panels B and C averages and standard deviations over four replicates are shown.

while for high peptide concentrations, a higher particle concentration is needed to obtain the same effect. At certain particle concentration, the reaction becomes so fast that the lag phase falls in a time range before the measurements start. After that concentration, the total fluorescence intensity at the plateau of the curve decreases significantly with respect to the traces in the absence of particles and at low particle concentrations. Several data sets at high nanoparticle concentration are biphasic (see, for example, data for 8 μM Aβ(M1−40) and 170 μg/mL nanoparticle in Figure 4A) but the amplitude of the early event devoid of a lag time decreases as the nanoparticle concentration is increased.

Our results imply that the nucleation of Aβ fibril formation is strongly disturbed by the presence of amino functionalized polystyrene nanoparticles and that the perturbation depends on the ratio between the peptide concentration and the nanoparticle surface area. The formation of amyloid fibrils is a phase separation process with all the characteristics of a nucleated polymerization reaction including an initial assembly of monomers into oligomers and formation of a critical nucleus and later elongation through monomer addition, and at the end of the process there are mature fibrils in equilibrium (extremely shifted toward the formation of fibrils) with soluble species (*17*−*19*). Within this framework, the lag time for the onset of fibrillation can be modified by disturbing the early stages of the process in a variety of manners. Additives may change the kinetics parameters in several qualitatively different, and to some degree independent, manners. First, perturbing the rates of formation and dissociation of early oligomers will increase or decrease the lag time, that is, the time to form critical nuclei that will lead to elongation. Second, modification of the rate of monomer addition to growing aggregates will alter the elongation rate. Third, trapping or deactivation of monomeric peptide will withdraw monomer from the reaction resulting in both a reduced number of critical nuclei at the early stages of the reaction and a reduced amount of fibrils at the later stages of the fibrillation process, resulting in a lower equilibrium plateau value. Addition of the nanoparticles clearly affects several of the underlying equilibria through interaction between nanoparticles and peptide; however, we cannot be sure at this stage whether the particles interact with the monomer, oligomers, or both.

If we analyze in detail the effect of amine-modified polystyrene nanoparticle concentration on the lag time of fibrillation, we can see that there is a jump in behavior, that is, a critical point. The transition between acceleration and inhibition is not a continuous process. On the contrary, there is a turnover concentration (or critical concentration) above which no catalysis of the process is observed and the addition of particles instead inhibits the fibrillation process. This is shown graphically in Figure 5. The half-times ($t_{1/2}$) for each individual replica for all the experiments performed under the same experimental conditions for 120 and 180 nm amino-modified polystyrene nanoparticles were calculated by fitting an empirical sigmoidal curve to the data (see Methods, eq 1). Since the elongation rate seems practically undisturbed, the variation in the overall rate depends mainly on the length of the lag time. Therefore, $t_{1/2}$ is directly proportional to the nucleation rate. A similar calculation has been made for the experiments investigating the fibrillation of Aβ(M1−40) or Aβ(M1−42) in the presence of 57 nm amine-modified polystyrene nanoparticles at different particle and peptide concentrations. To be able to compare the results for the three

DOI: 10.1021/cn900027u | *ACS Chem. Neurosci.* (2010), *1*, 279–287

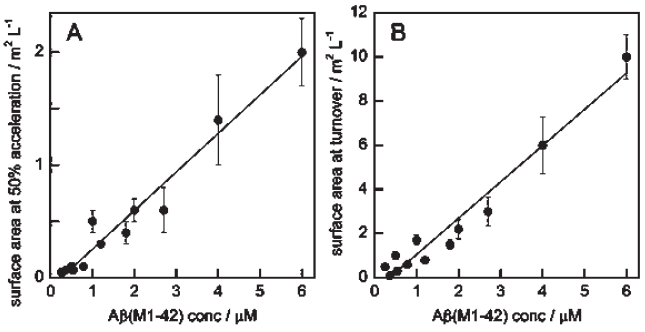

Figure 6. Nanoparticle surface area versus Aβ(M1−42) concentration for (A) the condition at which the half-time is reduced by 50% compared with the undisturbed case and (B) the turnover point defined as the last fibrillation curve that is not retarded relative to the undisturbed condition. Averages and standard deviations over three or four replicates are shown.

different particle sizes, the particle surface area in solution was calculated for each experimental condition, and $t_{1/2}$ was plotted versus the total surface area exposed by the nanoparticles in solution (Figure 5). The surface area calculation was made using the sizes obtained by dynamic light scattering, which do not differ greatly from the nominal values (58 ± 1, 127 ± 3, and 182 ± 2 nm). For biphasic curves, the $t_{1/2}$ values of both processes are reported.

For all three Aβ peptides, the behavior observed can be clearly divided into two classes: (i) shortening of the lag phase when the nanoparticle surface area in solution is less than the nanoparticle surface area turnover value and (ii) elongation of the lag phase when the nanoparticle surface area in solution is larger than the critical value, although during this regime the recombinant peptides show the coexistence of both the accelerated and retarded process.

The data for Aβ(M1−40) and Aβ(M1−42) fibrillation as a function of both peptide and nanoparticle concentration allow an analysis of the nanoparticle surface area required for the catalytic effect. The minimum particle surface area required to produce a significant acceleration of the fibrillation process was found to depend on the total concentration of peptide in solution. At low peptide concentration, a smaller particle surface area is required to accelerate the process than at a high peptide concentration (Figure 6A). For example, the particle surface area needed to reduce the half time of fibrillation by 50% with respect to the value observed in the absence of particles is approximately 2 m^2/L for a solution of 6 μM Aβ(M1−42). However, only 0.07 m^2/L of particle surface area is required to produce the same effect when the concentration of peptide concentration is reduced to 0.54 μM.

In the case of Aβ(1−40), the turnover value occurs around a nanoparticle surface area of 2.2 m^2/L (Figure 5A). A globular protein with the molecular weight of Aβ would have a diameter of 2 nm and a cross-sectional area of 3×10^{-18} m^2, whereas a partially unfolded peptide will have somewhat larger dimensions. Aβ(1−40) was studied at 8 μM; thus the total peptide cross-sectional area per liter of solution is 15 m^2/L for a globular protein and somewhat larger than that for a partially unfolded peptide. Notably, this is in the same order of magnitude as the exposed nanoparticle surface area. The critical point seems to occur at a peptide/particle surface area ratio at which the peptide concentration is still in excess over the amount required to form a single (mono)layer of adsorbed peptides on the nanoparticle surface. In the case of the recombinant peptides Aβ(M1−40) and Aβ(M1−42), the process was studied also as a function of peptide concentration and the turnover surface area is higher the higher the peptide concentration (Figure 5B,C). The total peptide cross-sectional area per liter of solution ranges between 0.4 and 11 m^2/L, and the turnover point ranges from 0.1 to 10 m^2/L when defined as the last point before the process is clearly retarded beyond the undisturbed condition or biphasic with the latter phase retarded beyond the undisturbed condition (Figure 6B). The surface area at the turnover point seems to scale linearly with the peptide concentration, and the values obtained indicate the need for formation of a single layer or less after the critical point, when inhibition becomes relevant. If the particles interact with oligomers, which present a smaller cross-sectional area per Aβ peptide unit, or bind more than a single layer, a majority of the peptide can be bound at and above the critical point. Acceleration of the elongation process thus seems to require that the peptide exchanges between the surface-bound and free forms with a significant peptide population being in the free state. Initiation of the fibrillation seems to depend on the interplay between intermolecular events catalyzed at the nanoparticle surface and events going on in solution. As long as there is a significant peptide population in solution, the process gets faster the more nanoparticle surface area that is available. Inhibition of the process starts to become relevant when the particle surface area in solution is sufficient to deplete a large fraction of the peptide from solution; therefore, the concentration and the aggregation of protein in solution is reduced leading to an inhibition of the fibrillation process. The differences observed in the minimum surface area of particle required to exert inhibition between the Aβ(1−40) and Aβ(M1−42) peptides could be a feature of the different aggregation propensities and physiochemical properties of the peptide. Aβ(M1−42) is more hydrophobic and aggregation prone than the shorter Aβ(1−40).

Another intriguing observation is that the ThT fluorescence intensity of the equilbrium plateau passes through a maximum at intermediate nanoparticle concentration

DOI: 10.1021/cn900027u | ACS Chem. Neurosci. (2010), 1, 279–287

Scheme 1

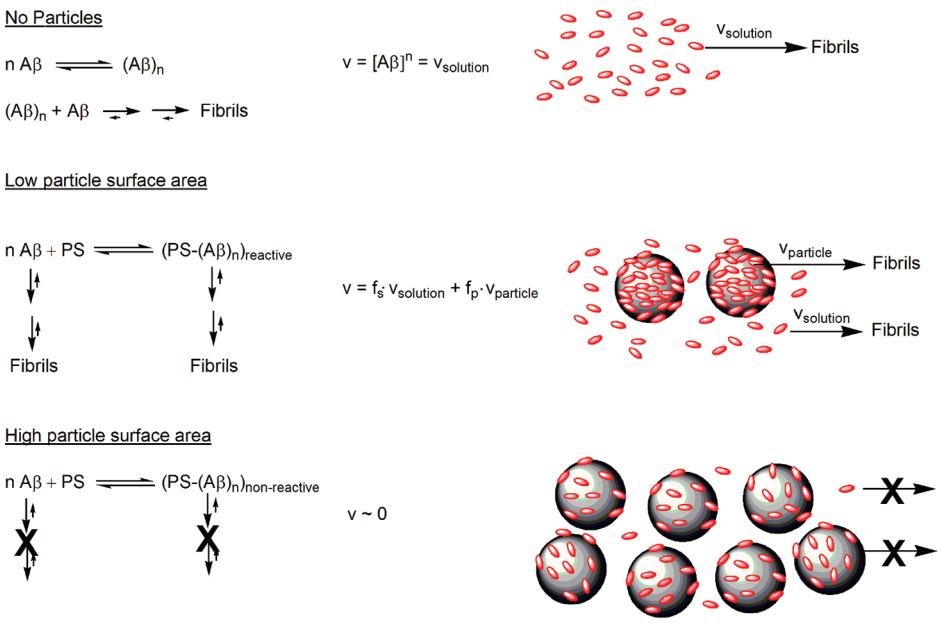

close to or just below the turnover concentration where the lag time vanishes (Figure 4A). This behavior is strikingly similar to that observed for α-synuclein aggregation as a function of SDS concentration, explained as different modes of interaction in different concentration regimes (*20*).

Our results clearly show that not only the total amount of nanoparticles is important, but the ratio between the peptide concentration and the nanoparticle surface area defines the behavior of the system. We can classify the experimental conditions into two regimes, with (i) high and (ii) low peptide concentration to surface area ratio. The dual effect of amine-modified polystyrene nanoparticles can be explained if we consider the presence and coexistence of at least two aggregation pathways (Scheme 1). The first pathway ($v = v_{solution}$) involves the formation of fibrils in solution and is the same process that occurs in the absence of nanoparticles. The second pathway ($v = v_{particle}$) involves the formation of critical nuclei and therefore seeds for fibrillation at the particle surface. The overall rate of fibrillation will depend on the interplay between the two pathways, and the predominance of one mechanism over the other will be determined by the relative equilibrium and rate constant in each case as well as the experimental conditions ($v = f_s v_{solution} + f_p v_{particle}$, where f_s and f_p are the fraction of peptide free in solution and adsorbed on the particle surface, respectively).

At high peptide to nanoparticle surface area ratio, a very large fraction of the peptide is in solution, and the first pathway dominates. Therefore we observe no effect on the peptide fibrillation rate at the lowest nanoparticle concentrations tested. The second pathway becomes more and more important as the nanoparticle concentration increases. Higher particle concentration will increase the fraction of peptide on the particle surface, and above a certain value, the contribution of the particle-catalyzed pathway will be significant to show an effect on the overall rate constant, and thus the reaction will proceed faster. This model requires that the reaction rate constant on the particle surface is higher than the one in solution. Therefore, for all peptide concentrations studied, there is a range of nanoparticle concentrations for which we see an acceleration of the overall process.

A third scenario takes over above the turnover concentration of nanoparticles, at which point the presence of the nanoparticles seems to inhibit both pathways. The first pathway is inhibited due to reduction of the concentration of Aβ in solution and the second by spreading the bound Aβ more thinly on the larger nanoparticle surface reducing Aβ's ability to oligomerize and nucleate the fibrillation process on the particle surface (Scheme 1). Recent studies of pure Aβ(M1−42) in solution have shown that the length of the lag phase depends on the local Aβ concentration to the power of -1.5 ($t_{lag} \approx c^{-1.5}$) (*19*); thus reducing the Aβ concentration in solution will have a large influence on the lag time for the first pathway. For example, a 50% reduction in peptide solution concentration increases the fibrillation lag time by a factor of 2.8.

The results of the present study imply that to reach mechanistic insights into the effect of nanoparticles on protein fibrillation, the process needs to be studied as a function of both protein and particle concentration.

DOI: 10.1021/cn900027u | *ACS Chem. Neurosci.* (2010), *1*, 279–287

Methods

Materials

Amyloid peptide Aβ(1−40) was synthesized by the W. M. Keck foundation, Biotechnology Resource Laboratory (Yale University), with an 80% purity (the remaining 20% of the lyophylized material is mainly water and some residual TFA). Correct mass was confirmed by matrix-assisted laser desorption/ionization time-of-flight mass spectroscopy. Recombinant Aβ(M1−42) was produced and purified as described elsewhere (*21*). Amino-modified polystyrene nanoparticles in three different nominal sizes, 57, 120, and 180 nm, were obtained from Bangs Laboratories. Other chemicals were from Aldrich.

ThT Fluorescence Assay

ThT fluorescence assays were conducted as described previously (*22*). Briefly, Aβ(1−40) was dissolved in a 50:50 mixture of 5% NH_4OH and 100 mM Tris buffer. Thereafter solutions were ultracentrifuged for 1 h at 1 000 000*g* and 4 °C in a Beckman ultracentrifuge in order to remove pre-existing amyloid fibrils. The upper 75% of the supernatant was collected, and the concentration of Aβ(1−40) was determined from the absorbance at 275 nm. The supernatant was then diluted to 8−16 μM with 12 mM sodium phosphate buffer, 0.02% NaN_3, pH 7.4. For the continuous experiments, 8 or 16 μM of Aβ(1−40) with 200 μM ThT was incubated in the absence or presence of nanoparticles (at several concentrations) at 37 °C and shaken at 700 rpm in a 96 well black fluorescence plate, NUNC 96 black polypropylene microwell plates, using a VorTemp 56 incubator/shaker with an orbit of 3 mm (Labnet International, Berkshire, U.K.). Measurements were made at regular intervals using a Molecular Devices SpectraMax M2 microplate reader (Sunnyvale, CA) with excitation and emission at 440 and 480 nm, respectively. Each experimental point is an average of the fluorescence signal from three to six wells containing aliquots of the same solution (same particle and protein concentration).

For experiments monitoring the effects of different particle injection times, 12 wells were filled with 90 μL of 8 μM Aβ(1−40) solution containing 200 μM ThT. The plate was placed in a VorTemp 56 incubator/shaker and monitored as described above. After 30 min, 10 μL of particle solution at 10 times the desired final concentration was added to the second well (first well had particles added at time zero), and the plate was read. Sequentially, particles were added to new wells every 30 min up to 300 min, and the fluorescence was monitored in all wells. After all the wells, except the particle-free control, had particles, the fluorescence was monitored until the reaction was finished, that is, when the fluorescence signal had reached a stable value in the no particle control samples.

In the case of Aβ(M1−40) or Aβ(M1−42), aliquots of purified peptide (*21*) were thawed and subjected to gel filtration on a Superdex 75 column in the experimental buffer (20 mM sodium phosphate buffer with 200 μM EDTA and 0.02% NaN_3 at pH 8.0 for Aβ(M1−42) and pH 7.4 for Aβ(M1−40)). The latter part of monomer peak was collected on ice, and the peptide concentration was determined by quantitative amino acid analysis (purchased from BMC Uppsala). The gel filtration step removes traces of pre-existing aggregates. The collected monomer was supplemented with 20 μM thioflavin T (ThT) from a 2 mM stock and was used at different dilutions in the respective experimental buffer supplemented with 20 μM ThT. The dilutions were made in tubes on ice using careful pipetting to avoid introduction of air bubbles. Twelve different concentrations of Aβ(M1−42) and five concentrations of Ab(M1−40) were studied. Peptide samples were pipetted into wells of a 96 well half-area plate of black polystyrene with a clear bottom and PEG coating (Corning 3881), 90 μL per well, which contained either 10 μL of buffer or 10 μL of amino-modified polystyrene nanoparticles (one of eleven different concentrations) resulting in final nanoparticle concentrations between 30 ng/mL and 1 mg/mL. The samples were added to the plate from lower to higher Aβ concentration after which the plate was sealed with a plastic film (Corning 3095). Four replicates were studied for each condition. The experiment was initiated by placing the 96-well plate at 37 °C with shaking at 100 rpm in a plate reader (Fluostar Omega, BMG Labtech, Offenburg, Germany). The ThT fluorescence was measured through the bottom of the plate every 6 min (with excitation filter 440 nm and emission filter 480 nm) with continuous shaking at 100 rpm between readings.

The experimental data were analyzed assuming a typical sigmoidal behavior in order to obtain the kinetics parameters of the bimodal fibrillation processes. An empirical sigmoidal equation was used (*23*, *24*)

$$Y = y_0 + \frac{y_{max} - y_0}{1 + e^{-(t - t_{1/2})k}} \quad (1)$$

In eq 1, y is the fluorescence intensity at time t, y_0 and y_{max} are the initial and maximum fluorescence intensities, respectively, $t_{1/2}$ is the time required to reach half the maximum intensity, and k is the apparent first-order aggregation constant.

Lag time is defined as

$$\text{lagtime} = t_{1/2} - 2/k \quad (2)$$

Transmission Electron Microscopy

Negative-staining EM was performed. The sample was applied to a carbon-coated Formvar grid, blotted with filter paper, allowed to dry for 2 min, stained with uranyl acetate 2% in water, blotted with filter paper and allowed to air-dry, and then viewed using a JEOL 2000 electron transmission microscope operated at 80 V. All reagents were supplied by Electron Microscopy Sciences (Hatfield, PA). Samples used for EM were prepared as described above from 16 μM Aβ(1−40) and 200 μM ThT at different incubations times.

Size Determination

Nanoparticle size measurements were performed using a Malvern Nanosizer ZS. Amino-modified polystyrene nanoparticles of nominal sizes 57, 120, and 180 nm were vortexed, sonicated for 5 min, and diluted to 0.125 mg/mL in 10 mM sodium phosphate buffer at pH 7.4 and equilibrated at 37 °C for 5 min before measurement took place. Ten measurements of each sample were taken using a clear disposable zeta cell at a backscatter angle of 173°. A general purpose analysis model was applied because this is deemed appropriate for most dispersions and emulsions.

DOI: 10.1021/cn900027u | *ACS Chem. Neurosci.* (2010), *1*, 279–287

Author Information

Corresponding Author

*E-mail addresses: celiacl@uvigo.es; Sara.Linse@biochemistry.lu.se.

Present Addresses

§ Present address: Departamento de Química Física, Facultade de Química, Universidade de Vigo, Campus Universitario Lagoas Marcosende s/n 36310 Vigo, Spain.

Author Contributions

C.C.-L. and S.L. designed the experiments. I.L., K.A.D., and S.L. provided materials. C.C.-L., F.Q.-P., and S.L. performed experiments. C.C.-L. and S.L. analyzed data and wrote the paper.

Funding Sources

Funding for the work was provided by Irish Research Council for Science, Engineering and Technology and the Xunta de Galicia (Programa de Recursos humanos do Plan Galego de Innovacion, Desenvolvemento e Teccnoloxia-INCITE Isidro Parga Pondal) (C.C.-L.), EPA Ph.D. fellowship 2007-FS-EH-7-M5-R2 (F.Q-P.), EU FP6 project NanoInteract (NMP4-CT-2006-033231) and SFI SRC BioNanoInteract (07 SRC B1155), the Swedish Research Council (VR) and its Linneaus Centre Organizing Molecular Matter (Lund, Sweden), and the Crafoord Foundation (Lund, Sweden).

References

1. Hardy, J., and Selkoe, D. J. (2002) Medicine - The amyloid hypothesis of Alzheimer's disease: Progress and problems on the road to therapeutics. *Science 297* (5580), 353–356.

2. Chiti, F., and Dobson, C. M. (2006) Protein misfolding, functional amyloid, and human disease. *Annu. Rev. Biochem. 75*, 333–366.

3. Necula, M., Kayed, R., Milton, S., and Glabe, C. G. (2007) Small molecule inhibitors of aggregation indicate that amyloid beta oligomerization and fibrillization pathways are independent and distinct. *J. Biol. Chem. 282* (14), 10311–10324.

4. Hughes, E., Burke, R. M., and Doig, A. J. (2000) Inhibition of toxicity in the beta-amyloid peptide fragment beta-(25−35) using N-methylated derivatives - A general strategy to prevent amyloid formation. *J. Biol. Chem. 275* (33), 25109–25115.

5. Ikeda, K., Okada, T., Sawada, S., Akiyoshi, K., and Matsuzaki, K. (2006) Inhibition of the formation of amyloid beta-protein fibrils using biocompatible nanogels as artificial chaperones. *FEBS Lett. 580* (28−29), 6587–6595.

6. Kim, J. E., and Lee, M. (2003) Fullerene inhibits beta-amyloid peptide aggregation. *Biochem. Biophys. Res. Commun. 303* (2), 576–579.

7. Linse, S., Cabaleiro-Lago, C., Xue, W. F., Lynch, I., Lindman, S., Thulin, E., Radford, S. E., and Dawson, K. A. (2007) Nucleation of protein fibrillation by nanoparticles. *Proc. Natl. Acad. Sci. U.S.A. 104* (21), 8691–8696.

8. Cabaleiro-Lago, C., Quinlan-Pluck, F., Lynch, I., Lindman, S., Minogue, A. M., Thulin, E., Walsh, D. M., Dawson, K. A., and Linse, S. (2008) Inhibition of amyloid beta protein fibrillation by polymeric nanoparticles. *J. Am. Chem. Soc. 130* (46), 15437–15443.

9. Wu, W. H., Sun, X., Yu, Y. P., Hu, J., Zhao, L., Liu, Q., Zhao, Y. F., and Li, Y. M. (2008) TiO2 nanoparticles promote beta-amyloid fibrillation in vitro. *Biochem. Biophys. Res. Commun. 373* (2), 315–318.

10. Klajnert, B., Cortijo-Arellano, M., Cladera, J., and Bryszewska, M. (2006) Influence of dendrimer's structure on its activity against amyloid fibril formation. *Biochem. Biophys. Res. Commun. 345*, 21–28.

11. Sluzky, V., Tamada, J. A., Klibanov, A. M., and Langer, R. (1991) Kinetics of insulin aggregation in aqueous-solutions upon agitation in the presence of hydrophobic surfaces. *Proc. Natl. Acad. Sci. U.S.A. 88* (21), 9377–9381.

12. Rocha, S., Thuneman, A. F., Pereira, M. D., Coelho, M., Mohwald, H., and Brezesinski, G. (2008) Influence of fluorinated and hydrogenated nanoparticles on the structure and fibrillogenesis of amyloid beta-peptide. *Biophys. Chem. 137* (1), 35–42.

13. Giacomelli, C. E., and Norde, W. (2005) Conformational changes of the amyloid beta-peptide (1−40) adsorbed on solid surfaces. *Macromol. Biosci. 5* (5), 401–407.

14. Walsh, D. M., and Selkoe, D. J. (2004) Deciphering the molecular basis of memory failure in Alzheimer's disease. *Neuron 44* (1), 181–193.

15. Levine, H. (1995) Thioflavine-T interaction with amyloid beta-sheet structures. *Amyloid 2* (1), 1–6.

16. Cabaleiro-Lago, C., Lynch, I., Dawson, K. A., and Linse, S. (2009) Inhibition of IAPP and IAPP(20−29) fibrillation by polymeric nanoparticles. *Langmuir*, published online December 17, DOI 10.1021/la902980d.

17. Ferrone, F., Analysis of protein aggregation kinetics. In *Methods in Enzymology*, Academic Press Inc.: 1999; Vol. 309, pp 256−274.

18. Xue, W. F., Homans, S. W., and Radford, S. E. (2008) Systematic analysis of nucleation-dependent polymerization reveals new insights into the mechanism of amyloid self-assembly. *Proc. Natl. Acad. Sci. U.S.A. 105* (26), 8926–8931.

19. Hellstrand, E., Boland, B., Walsh, D. M., and Linse, S. (2009) Amyloid β-protein aggregation produces highly reproducible kinetic data and occurs by a two-phase process. *ACS Chem. Neurosci. 1*, 13–18.

20. Giehm L; Oliviera C. L. P.; Christiansen G; Pedersen J. S.; D, O. SDS-induced fibrillation of α-synuclein: An alternative fibrillation pathway. *J. Mol. Biol.*, submitted for publication.

21. Walsh, D. M., Thulin, E., Minogue, A. M., Gustavsson, N., Pang, E., Teplow, D. B., and Linse, S. (2009) A facile method for expression and purification of the Alzheimer's disease-associated amyloid beta-peptide. *FEBS J. 276* (5), 1266–1281.

22. Betts, V., Leissring, M. A., Dolios, G., Wang, R., Selkoe, D. J., and Walsh, D. M. (2008) Aggregation and catabolism of disease-associated intra-A beta mutations: Reduced proteolysis of A beta A21G by neprilysin. *Neurobiol. Dis. 31* (3), 442–450.

23. Nielsen, L., Khurana, R., Coats, A., Frokjaer, S., Brange, J., Vyas, S., Uversky, V. N., and Fink, A. L. (2001) Effect of environmental factors on the kinetics of insulin fibril formation: Elucidation of the molecular mechanism. *Biochemistry 40* (20), 6036–6046.

24. Kodaka, M. (2004) Requirements for generating sigmoidal time-course aggregation in nucleation-dependent polymerization model. *Biophys. Chem. 107* (3), 243–253.

DOI: 10.1021/cn900027u | *ACS Chem. Neurosci.* (2010), *1*, 279–287